

No or Diffuse Phase-Transition With Temperature in One-dimensional Ising Model?

Li Zhang

Nanjing University

Li-Li Zhang

Nanjing University

Yi-Neng Huang (✉ ynhuang@nju.edu.cn)

Nanjing University <https://orcid.org/0000-0002-2031-4395>

Article

Keywords: Phase-Transition, heterogeneous, spontaneous-magnetization

Posted Date: May 27th, 2021

DOI: <https://doi.org/10.21203/rs.3.rs-516637/v1>

License: © ⓘ This work is licensed under a Creative Commons Attribution 4.0 International License.

[Read Full License](#)

No or diffuse phase-transition with temperature in one-dimensional Ising model?

Li Zhang^{1,2}, Li-Li Zhang¹, and Yi-Neng Huang^{1,2*}

¹National Laboratory of Solid State Microstructures, School of Physics, Nanjing University, China.
²Xinjiang Laboratory of Phase Transitions and Microstructures in Condensed Matters, College of Physical Science and Technology, Yili Normal University, China. *Corresponding author. Email: ynhuang@nju.edu.cn

Abstract

For nearly a century since Ising model was proposed in 1925, it is agreed that there is no phase-transition with temperature in the one-dimensional based on no global-spontaneous-magnetization in whole temperature region. In this letter, the exact calculation of local-spontaneous-magnetization shows that a diffuse phase-transition with temperature occurs in one-dimensional Ising model. In addition, although diffuse phase-transition phenomenon is common in the systems of heterogeneous-components and small-sizes etc., there is no accurate prediction of corresponding theoretical models so far, so the present works lay the theoretical foundation of this kind of phase-transition.

In the nearly 100 years since Ising model (IM)¹, one of the most important microscopic models of phase-transition²⁻⁸, was proposed in 1925, it is agreed that there is no temperature dependent phase-transition in the one-dimensional. This is because the global-spontaneous-magnetization of the model system is zero in whole temperature range, i.e. there is no global-spontaneous-magnetization^{1,2} as shown in the Supplementary Information (SI).

However, the absence of global-spontaneous-magnetization does not deny the existence of short-range local-spontaneous-magnetization in one-dimensional-IM (1D-IM). In this paper, the local-spontaneous-magnetization with temperature and size in the model is calculated accurately, and the results show that 1D-IM has a diffuse phase-transition with temperature⁹⁻¹³. In other words, our conclusion subverts the century consensus in this model.

Results

The Hamiltonian (H_{1D-IM}) of one-dimensional Ising model (1D-IM) is,

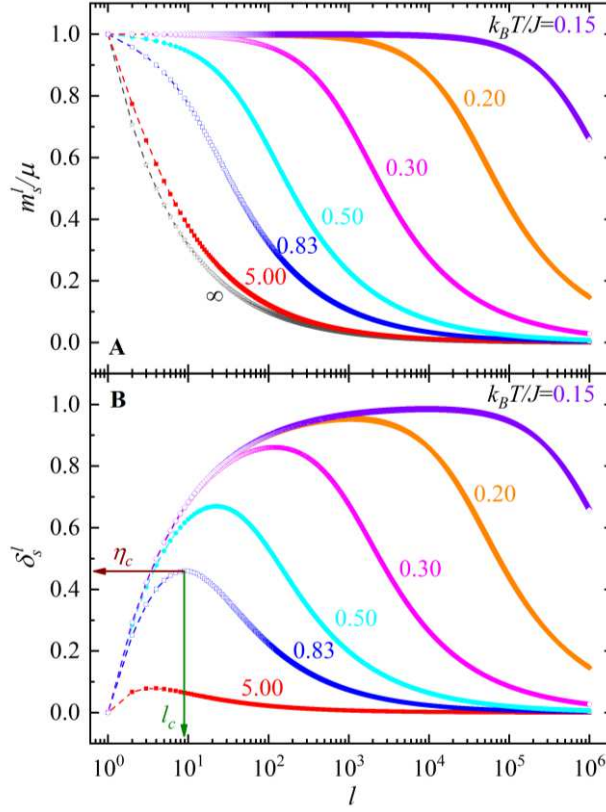
$$H_{1D-IM} = \lim_{N \rightarrow \infty} \left[-J \sum_{i=1}^{N-1} \sigma_i \sigma_{i+1} \right] \quad (1)$$

in which σ_i is the i th spin and $\sigma_i = \pm 1$, J the interaction energy constant between the nearest-neighbor spins, and N the total number of spins in the model system (Fig. S1).

In the model, the local magnetic moment (s_l^r) including l nearest-neighbor spins is,

$$s_l^r \equiv \mu \sum_{i=0}^{l-1} \sigma_{r+i} \quad (2)$$

where μ is the magnetic moment of a spin, and r expresses an arbitrary reference site.



40

41 Fig. 1. For series T , (A) local-spontaneous-magnetization (m_s^l) and (B) relative local-
 42 spontaneous-magnetization (δ_s^l) vs local spin number (l) in one-dimensional Ising
 43 model.

44

45 To describe the temperature dependence of the amplitude of s_i^r (excluding the orientations
 46 corresponding to its signs) in this paper, the local-spontaneous-magnetization (m_s^l) is defined
 47 as (see SI and METHODS),

$$\begin{aligned}
 m_s^l &\equiv \frac{1}{l} \sqrt{\lim_{n \rightarrow \infty} \frac{1}{Z_n} \sum_{\sigma_i = \pm 1, \dots, \sigma_n = \pm 1} (s_i^r)^2 \exp \left[\frac{J}{k_B T} \sum_{i=1}^{n-1} \sigma_i \sigma_{i+1} \right]} \\
 &= \frac{\mu}{l} \sqrt{2 \left[\frac{l - \gamma^l}{1 - \gamma} - \frac{\gamma(1 - \gamma^{l-1})}{(1 - \gamma)^2} \right] - l}
 \end{aligned} \tag{3}$$

48

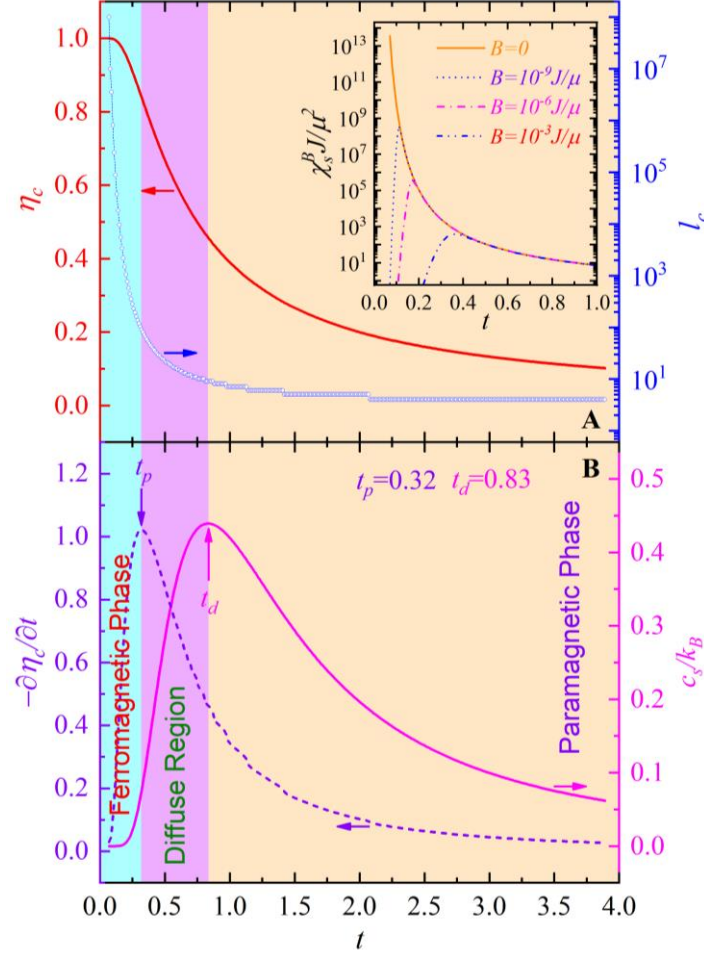
49 here k_B is Boltzmann constant, T the temperature of the heat bath in which the one-
 50 dimensional spin chain is located, Z_n the partition function of the spin orientation ensemble of
 51 1D-IM (SI), and n the spin number of the subsystems in the ensemble (Fig. S1), and $\gamma \equiv$
 52 $\tanh\left(\frac{J}{k_B T}\right)$.

53 Obviously, m_s^∞ is the global stochastic magnetization when $l \rightarrow \infty$. From Eq. 3, we can
 54 get that $m_s^\infty = 0$ except $T \rightarrow 0$, which is consistent with the past result^{1,2}.

55 Fig. 1A shows m_s^l vs l for series T , and it can be seen that: (i) At high temperature (e.g.
 56 $T = 5.00J/k_B$), m_s^l decreases rapidly with increasing l , which indicates that the spatial scale

57
58
59
60

of local-spontaneous-magnetization is small; and (ii) At low temperature (e.g. $T = 0.15J/k_B$), $m_s^l \rightarrow \mu$ in a large range of l , which states clearly that the local-spontaneous-magnetization regions not only has a large spatial scale, but also almost all the spins in the regions have the same orientation.



61

Fig. 2. (A) characteristic spontaneous magnetization (η_c) and its characteristic spatial size (l_c), as well as (B) $-\partial\eta_c/\partial t$ and heat capacity per spin (c_s) in 1D-IM vs reduced temperature ($t \equiv k_B T/J$). Inset of Fig. 2A shows static susceptibility (χ_s^B) per spin vs t for a series of external magnetic fields (B).

62

Discussion

63

According to Landau theory¹⁴, the order parameter is the essential to phase-transition, which characterizes the relative change of the low to high temperature phase. Therefore, in order to describe the relative variation of m_s^l to $m_s^l(T \rightarrow \infty)$, the relative local-spontaneous-magnetization (δ_s^l) is introduced here,

64

$$\delta_s^l \equiv \frac{m_s^l - m_s^l(T \rightarrow \infty)}{\mu} \quad (4)$$

65

In fact, $m_s^l(T \rightarrow \infty)$ represents the autocorrelation (σ_i^2) of a spin (Eq. 3 and M5 in METHODS), and of course has nothing to do with the phase transition process.

66

At series T , δ_s^l vs l is shown in Fig. 1B, which indicates that for all temperatures, δ_s^l has a single diffuse peak as a function of l . In this paper, the maximum value of δ_s^l is expressed as

67

77 η_c , and the corresponding value of l as l_c . Obviously, η_c and l_c can be used as the
 78 characteristic parameters to describe the local-spontaneous-magnetization and its spatial size,
 79 so here η_c is called the characteristic spontaneous magnetization and l_c the characteristic
 80 spatial size of η_c in 1D-IM. Moreover, the dispersion of the δ_s^l peak shows that both the size
 81 of the local-spontaneous-magnetization regions and its internal magnetization have obvious
 82 distributions.

83 η_c and l_c vs T (Fig. 2A) show that with decreasing T : (i) η_c first increases slowly, then
 84 rapidly, and slowly again. It should be noted that at high temperature, η_c is still not zero (e.g.
 85 $\eta_c = 0.10$ when $T = 3.82J/k_B$). In addition, $\eta_c \rightarrow 1$ at nonzero low temperature (e.g. $\eta_c =$
 86 0.9999 for $T = 0.07J/k_B$); and (ii) l_c first increases slowly and then rapidly. For example,
 87 $l_c = 4$ when $T = 3.82J/k_B$, and $l_c = 10^8$ for $T = 0.07J/k_B$ (if the lattice parameter of 1D-
 88 IM is assumed to be 0.5 nanometers, the characteristic size of the local-spontaneous-
 89 magnetization region will reach the macroscopic ~ 5 centimeters). These results state clearly
 90 that in 1D-IM, there exists a diffuse transition between the nanoscale regions of small
 91 spontaneous magnetization at high temperature and the macroscopic domains of large
 92 spontaneous magnetization at low temperature.

93 By comparing the order parameters¹⁰⁻¹³, heat capacity¹⁵⁻¹⁷, and domain structure
 94 evolution¹⁸⁻²⁰ of existing diffuse phase-transition, with the diffuse variation of η_c , the diffuse
 95 peak^{1,2} of heat capacity (c_s) per spin (SI and Fig. 2B), and the diffuse transition between the
 96 nanoscale regions of local-spontaneous-magnetization to the macroscopic domains as a
 97 function of T , it can be concluded that a diffuse phase-transition with temperature occurs in
 98 1D-IM.

99 According to the method of reference²¹, the temperature corresponding to the maximum
 100 of $-\frac{\partial \eta_c}{\partial T}$ is defined as the characteristic temperature (T_p) of diffuse phase-transition in 1D-IM,
 101 and it is obtained $T_p = 0.32J/k_B$ (Fig. 2B). It should be pointed out that T_p is lower than the
 102 peak temperature ($T_d = 0.83J/k_B$) of c_s . For second-order or continuous phase-transition, the
 103 peak temperatures of heat capacity and the negative of the differential of order parameter to T
 104 are equal to each other^{14,22,23}, so the authors thinks that the difference between T_p and T_d just
 105 reflects the dispersion of the diffuse phase-transition. In order to describe this dispersion, the
 106 dispersion degree (φ) of the diffuse phase-transition is proposed as,

$$107 \quad \varphi \equiv \frac{T_d - T_p}{T_d + T_p} = 0.44 \quad (5)$$

108 It is worth noting that the static susceptibility (χ_s) per spin in 1D-IM (inset of Fig. 2A and
 109 SI) always increases rapidly with decreasing T ^{1,2}, instead of the λ -type peak of second-order
 110 phase-transition¹⁴, which is thought to be one of the key evidences that no phase-transition with
 111 temperature exist in this model.

112 In order to further explore the micro mechanism of the above characteristic of χ_s , the
 113 static susceptibility (χ_s^B) per spin in 1D-IM as a function of T in a fixed external magnetic field
 114 (B) is calculated (SI), as shown in the inset of Fig. 2A. We can see that for finite small B , there
 115 is a single diffuse peak of χ_s^B with T , and the peak temperature moves to high temperature with
 116 the increase of B . This is due to that very small B can saturate the magnetization of 1D-IM at
 117 low temperature (as shown in Fig. S2, the saturation $B \sim 10^{-9} J/\mu$ for $T = 0.10J/k_B$), while
 118 the saturated magnetization leads to a smaller value χ_s^B . Because the saturation magnetization
 119 corresponds to the single domain state of the model, the increase of χ_s at low temperature is
 120 caused by the movement of domain walls^{24,25}.

121 In particular, because the measurement magnetic field used in experiments is always finite,
 122 the susceptibility peak (inset of Fig. 2A) will appear in 1D-IM as long as the experimental
 123 measurement is carried out. In other words, the continuously increasing characteristic of the
 124 theoretically predicted χ_s ($\chi_s^{B=0}$) with decreasing T cannot be measured directly, which is only
 125 ideal value.

126 Although diffuse phase-transition is common in component-heterogeneous^{10-13,26-29} and
 127 small-size³⁰⁻³² systems, there is no accurate calculation of the corresponding theoretical model
 128 so far²¹. Therefore, the exact results in this paper lay the theoretical foundation of this kind of
 129 phase-transition.

130 Weiss mean-field theory³³ is always thought to be not suitable for 1D-IM because it
 131 predicts that there is a phase-transition with T in this system. The present and relevant^{2,22,23}
 132 results show that this theory is valid for IM of all dimensions in judging whether there exists
 133 phase-transition, although its predicting phase-transition behaviors, such as the transition
 134 temperature and the subtle characteristics of order parameter and heat capacity, are different
 135 from the exact solutions^{2,22,23}. It also shows that Weiss-type mean-field approximation²¹ is an
 136 effective and feasible method for Ising-category models of phase-transition which are too
 137 complex and difficult to get their exact solutions.

138 Traditionally, the description to 1st and 2nd-order phase-transitions is based on global-
 139 order-parameter (such as global-spontaneous-magnetization and global-spontaneous-
 140 polarization etc.)^{1,2,14,33}, but it cannot describe the spatially heterogeneous behavior of the
 141 order-parameter corresponding to the diffuse-phase-transition in component-heterogeneous<sup>10-
 142 13,26-29</sup> and small-size³⁰⁻³² systems. Obviously, as the scale of the local-order-parameter
 143 proposed in Ref.21 and this paper tends to infinity, it becomes the global-order-parameter. So,
 144 local-order-parameter can provide a unified description of 1st and 2nd-order phase-transitions
 145 as well as diffuse-phase-transition.

147 Methods

148 The method to calculate the local-spontaneous-magnetization (m_s^l) in 1D-IM is as the
 149 follows.

150 The Hamiltonian (H_n) of the subsystem (Fig. S1) without external magnetic field is,

$$151 \quad H_n = -J \sum_{i=1}^{n-1} \sigma_i \sigma_{i+1} \quad (\text{M1})$$

152 and the partition function (Z_n) of the spin orientation ensemble (Fig. S1) is,

$$153 \quad Z_n \equiv \sum_{\sigma_i=\pm 1, \dots, \sigma_n=\pm 1} \exp \left[v \sum_{i=1}^{n-1} \sigma_i^1 \sigma_{i+1}^1 \right] = \cosh^{n-1}(v) Q_n \quad (\text{M2})$$

154 In which,

$$155 \quad Q_n \equiv \sum_{\sigma_i=\pm 1, \dots, \sigma_n=\pm 1} \prod_{i=1}^{n-1} (1 + \gamma \sigma_i \sigma_{i+1}) = 2^n \quad (\text{M3})$$

156 Let,

$$157 \quad X_l \equiv \lim_{n \rightarrow \infty} \frac{1}{Z_n} \sum_{\sigma_i=\pm 1, \dots, \sigma_n=\pm 1} (s_l^r)^2 \exp \left[v \sum_{i=1}^{n-1} \sigma_i \sigma_{i+1} \right] \quad (\text{M4})$$

158 and according to,

$$(s_l^r)^2 = \mu^2 \left\{ l + 2 \left[\sum_{i=1}^{l-1} \sigma_{r+i-1}^1 \sigma_{r+i}^1 + \sum_{i=2}^{l-1} \sigma_{r+i-2}^1 \sigma_{r+i}^1 + \cdots + \sum_{i=l-1} \sigma_r^1 \sigma_{r+l-1}^1 \right] \right\} \quad (\text{M5})$$

160 we obtain,

$$X_l = \mu^2 \left[l + 2 \sum_{k=1}^{l-1} (l-k) \zeta_k \right] \quad (\text{M6})$$

162 where ζ_k is the correlation function between σ_r and σ_{r+k} , i.e.

$$\begin{aligned} \zeta_k &\equiv \lim_{n \rightarrow \infty} \frac{1}{Z_n} \sum_{\sigma_i = \pm 1, \dots, \sigma_n = \pm 1} \sigma_r \sigma_{r+k} \exp \left[v \sum_{i=1}^{n-1} \sigma_i \sigma_{i+1} \right] \\ &= \lim_{n \rightarrow \infty} \frac{1}{Q_n} \sum_{\sigma_i = \pm 1, \dots, \sigma_n = \pm 1} \prod_{i=1}^{n-1} (1 + \gamma \sigma_i \sigma_{i+1}) \sigma_r \sigma_{r+k} \end{aligned} \quad (\text{M7})$$

164 Based on,

$$I_0 \equiv \sum_{\sigma_r = \pm 1} (1 + \gamma \sigma_{r-1} \sigma_r) (1 + \gamma \sigma_r \sigma_{r+1}) \sigma_r \quad (\text{M8})$$

$$\begin{aligned} &= 2\gamma(\sigma_{r-1} + \sigma_{r+1}) \\ I_1 &\equiv \sum_{\sigma_{r+1} = \pm 1} I_0 (1 + \gamma \sigma_{r+1} \sigma_{r+2}) \quad (\text{M9}) \\ &= 2^2 \gamma (\sigma_{r-1} + \gamma \sigma_{r+2}) \end{aligned}$$

$$\dots$$

$$\begin{aligned} I_k &\equiv \sum_{\sigma_{r+k} = \pm 1} I_{k-1} (1 + \gamma \sigma_{r+k} \sigma_{r+k+1}) \sigma_{r+k} \\ &= 2^{k+1} \gamma (\gamma^{k-1} + \gamma \sigma_{r-1} \sigma_{r+k+1}) \end{aligned} \quad (\text{M10})$$

169 we get,

$$\begin{aligned} \zeta_k &= \lim_{n \rightarrow \infty} \frac{1}{Q_n} \sum_{\substack{\sigma_i = \pm 1, \dots, \sigma_{r-1} = \pm 1 \\ \sigma_{r+k+1} = \pm 1, \dots, \sigma_n = \pm 1}} I_k \prod_{i=1}^{r-2} (1 + \gamma \sigma_i \sigma_{i+1}) \prod_{i=r+k+1}^{n-1} (1 + \gamma \sigma_i \sigma_{i+1}) \\ &= \gamma^k \end{aligned} \quad (\text{M11})$$

171 From Eq.M6 and M11, we obtain,

$$X_l = \mu^2 \left[l + 2 \sum_{k=1}^{l-1} (l-k) \gamma^k \right] \quad (\text{M12})$$

173 Here, $\sum_{k=1}^{l-1} (l-k) \gamma^k$ is the well-known arithmetic-geometric series, and,

$$X_l = \mu^2 \left\{ 2 \left[\frac{l - \gamma^l}{1 - \gamma} - \frac{\gamma(1 - \gamma^{l-1})}{(1 - \gamma)^2} \right] - l \right\} \quad (\text{M13})$$

175 Therefore,

$$m_s^l = \frac{\mu}{l} \sqrt{2 \left[\frac{l - \gamma^l}{1 - \gamma} - \frac{\gamma(1 - \gamma^{l-1})}{(1 - \gamma)^2} \right] - l} \quad (\text{M14})$$

177 and obviously,

$$m_s^l(T \rightarrow \infty) = \frac{\mu}{l^{1/2}} \quad (\text{M15})$$

179

180 **Data availability**

181 The data that support the plots and other findings of this paper are available from the
182 corresponding author upon a reasonable request.

183

184 Code availability

185 The code is available from the corresponding author upon a reasonable request.

186

187

References

- 188 1. Ising, E. Report on the theory of ferromagnetism. *Z. Phys.* **31**, 253-258 (1925).
- 189 2. McCoy, B. M. & Wu, T. T. *The two-dimensional Ising model*. (Dover Publications, Inc., Mineola, New
190 York, 2014).
- 191 3. Li, Y. Ising model for strings. *Nat. Phys.* **16**, 1006 (2020).
- 192 4. Young, J. T., Gorshkov, A. V., Foss-Feig, M. & Maghrebi, M. F. Nonequilibrium Fixed Points of
193 Coupled Ising Models. *Phys. Rev. X* **10**, (2020).
- 194 5. Christiansen, H., Majumder, S., Henkel, M. & Janke, W. Aging in the Long-Range Ising Model. *Phys.*
195 *Rev. Lett.* **125**, (2020).
- 196 6. Walker, N., Tam, K. & Jarrell, M. Deep learning on the 2-dimensional Ising model to extract the
197 crossover region with a variational autoencoder. *Sci. Rep.* **10**, (2020).
- 198 7. Wang, B., Hu, F., Yao, H. & Wang, C. Prime factorization algorithm based on parameter optimization
199 of Ising model. *Sci. Rep.* **10**, (2020).
- 200 8. Imanaka, Y., Anazawa, T., Kumasaka, F. & Jippo, H. Optimization of the composition in a composite
201 material for microelectronics application using the Ising model. *Sci. Rep.* **11**, (2021).
- 202 9. Smolenskii, G. A., Isupov, V. A., Agranovskaya, A. I. & Krainik, N. N. New ferroelectrics of complex
203 composition. *Sov. Phys. Sol. Stat.* **2**, 2651-2654 (1961).
- 204 10. Kimura, T., Tomioka, Y., Kumai, R., Okimoto, Y. & Tokura, Y. Diffuse phase transition and phase
205 separation in Cr-doped $\text{Nd}_{1/2}\text{Ca}_{1/2}\text{MnO}_3$: A relaxor ferromagnet. *Phys. Rev. Lett.* **83**, 3940-3943 (1999).
- 206 11. Granzow, T., Woike, T., Wohlecke, M., Imlau, M. & Kleemann, W. Change from 3D-Ising to random
207 field-Ising-model criticality in a uniaxial relaxor ferroelectric. *Phys. Rev. Lett.* **92**, 65701 (2004).
- 208 12. Gehring, P. M. et al. Reassessment of the Burns temperature and its relationship to the diffuse scattering,
209 lattice dynamics, and thermal expansion in relaxor $\text{Pb}(\text{Mg}_{1/3}\text{Nb}_{2/3})\text{O}_3$. *Phys. Rev. B* **79**, 224109 (2009).
- 210 13. Stock, C. et al. Interplay between static and dynamic polar correlations in relaxor $\text{Pb}(\text{Mg}_{1/3}\text{Nb}_{2/3})\text{O}_3$.
211 *Phys. Rev. B* **81**, 144127 (2010).
- 212 14. Landau, L. Zur Theorie der Phasenumwandlungen II. *Phys. Z. Soviet Union*. **545**, 26-35 (1937).
- 213 15. Moriya, Y., Kawaji, H., Tojo, T. & Atake, T. Specific-heat anomaly caused by ferroelectric nanoregions
214 in $\text{Pb}(\text{Mg}_{1/3}\text{Nb}_{2/3})\text{O}_3$ and $\text{Pb}(\text{Mg}_{1/3}\text{Ta}_{2/3})\text{O}_3$ relaxors. *Phys. Rev. Lett.* **90**, 205901 (2003).
- 215 16. Kleemann, W., Dec, J., Shvartsman, V. V., Kutnjak, Z. & Braun, T. Two-dimensional Ising model
216 criticality in a three-dimensional uniaxial relaxor ferroelectric with frozen polar nanoregions. *Phys. Rev.*
217 *Lett.* **97**, 65702 (2006).
- 218 17. Tachibana, M., Sasame, K., Kawaji, H., Atake, T. & Takayama-Muromachi, E. Thermal signatures of
219 nanoscale inhomogeneities and ferroelectric order in $[\text{PbZn}_{1/3}\text{Nb}_{2/3}\text{O}_3]_{1-x}[\text{PbTiO}_3]_x$. *Phys. Rev. B* **80**,
220 94115 (2009).
- 221 18. Burns, G. & Scott, B. A. Index of refraction in dirty displacive ferroelectrics. *Sol. State Commun.* **13**,
222 423-426 (1973).
- 223 19. Shvartsman, V. V. & Lupascu, D. C. Lead-free relaxor ferroelectrics. *J. Am. Cera. Soc.* **95**, 1-26 (2012).
- 224 20. Shvartsman, V. V., Dkhil, B. & Kholkin, A. L. Mesoscale domains and nature of the relaxor state by
225 piezoresponse force microscopy. *Annu. Rev. Mater. Res.* **43**, 423-449 (2013).
- 226 21. Zhang, L. L. & Huang, Y. N. Theory of relaxor-ferroelectricity. *Sci. Rep.* **10**, 50601 (2020).
- 227 22. Onsager, L. Crystal statistics I: A two-dimensional model with an order-disorder transition. *Phys. Rev.*
228 **65**, 117-149 (1944).
- 229 23. Yang, C. N. The spontaneous magnetization of a 2-dimensional Ising model. *Phys. Rev.* **85**, 808-815
230 (1952).
- 231 24. Huang, Y. N., Wang, Y. N. & Shen, H. M. Internal-friction and dielectric loss related to domain-walls.
232 *Phys. Rev. B* **46**, 3290-3295 (1992).
- 233 25. Huang, Y. N. et al. Domain freezing in potassium dihydrogen phosphate, triglycine sulfate, and
234 CuAlZnNi . *Phys. Rev. B* **55**, 16159-16167 (1997).
- 235 26. Cross, L. E. Relaxor ferroelectrics. *Ferroelectrics*. **76**, 241-267 (1987).
- 236 27. Kumar, A. et al. Atomic-resolution electron microscopy of nanoscale local structure in lead-based relaxor
237 ferroelectrics. *Nat. Mat.* **20**, (2021).

- 238 28. Li, F. et al. Giant piezoelectricity of Sm-doped Pb(Mg_{1/3}Nb_{2/3})O₃-PbTiO₃ single crystals. *Science*.
239 **364**, 264 (2019).
240 29. Krogstad, M. J. et al. The relation of local order to material properties in relaxor ferroelectrics. *Nat.*
241 *Mater.* **17**, 718-724 (2018).
242 30. Chattopadhyay, S., Ayyub, P., Palkar, V. R. & Multani, M. Size-induced diffuse phase-transition in the
243 nanocrystalline ferroelectric PbTiO₃. *Phys. Rev. B*. **52**, 13177-13183 (1995).
244 31. Muthuselvam, I. P. & Bhowmik, R. N. Grain size dependent magnetization, electrical resistivity and
245 magnetoresistance in mechanically milled La_{0.67}Sr_{0.33}MnO₃. *J. Alloys Comp.* **511**, 22-30 (2012).
246 32. Li, J. et al. Scale-invariant magnetic textures in the strongly correlated oxide NdNiO₃. *Nat. Commun.*
247 **10**, (2019).
248 33. Weiss, P. Molecular field and ferro-magnetism. *Phys. Z.* **9**, 358-367 (1908).
249

250 **Acknowledgments**

251 We sincerely thanks Prof. W. Kleemann, M. E. Manley and J. Petzelt for their enlightening
252 discussions on the mechanism of diffuse phase-transition. This work is supported by National
253 Natural Science Foundation of China (Grant No. 11664042).
254

255 **Author contributions**

256 Y-N.H. and L-L.Z. conceived this article together. Y-N.H. calculated the local-spontaneous-
257 magnetization. L.Z. did the numerical calculations and made plots.
258

259 **Competing interests**

260 Authors declare that they have no competing interests.
261

262 **Additional information**

263 All data are available in the main text or the supplementary information.
264

Figures

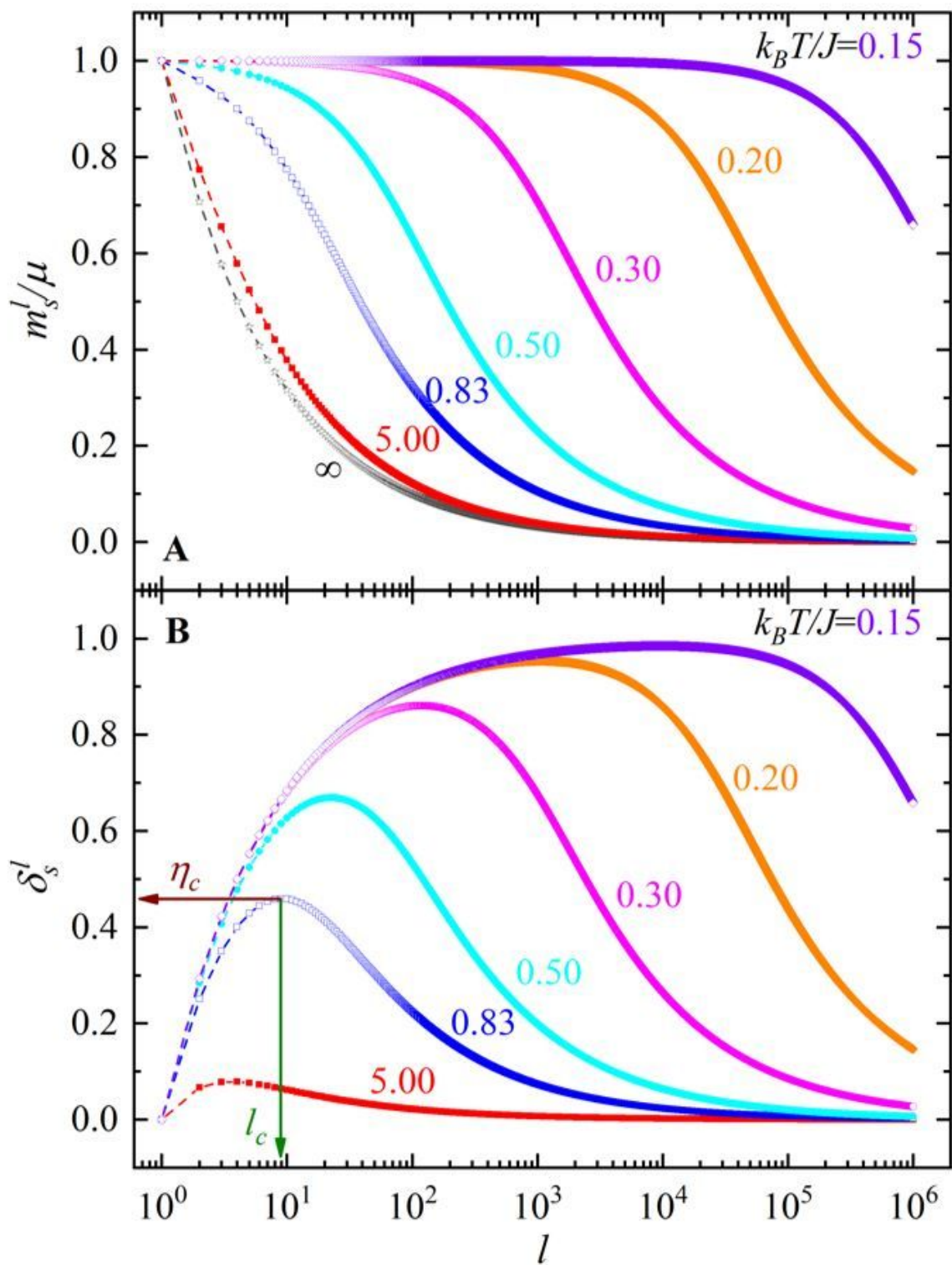


Figure 1

Please see the Manuscript file for the complete figure caption.

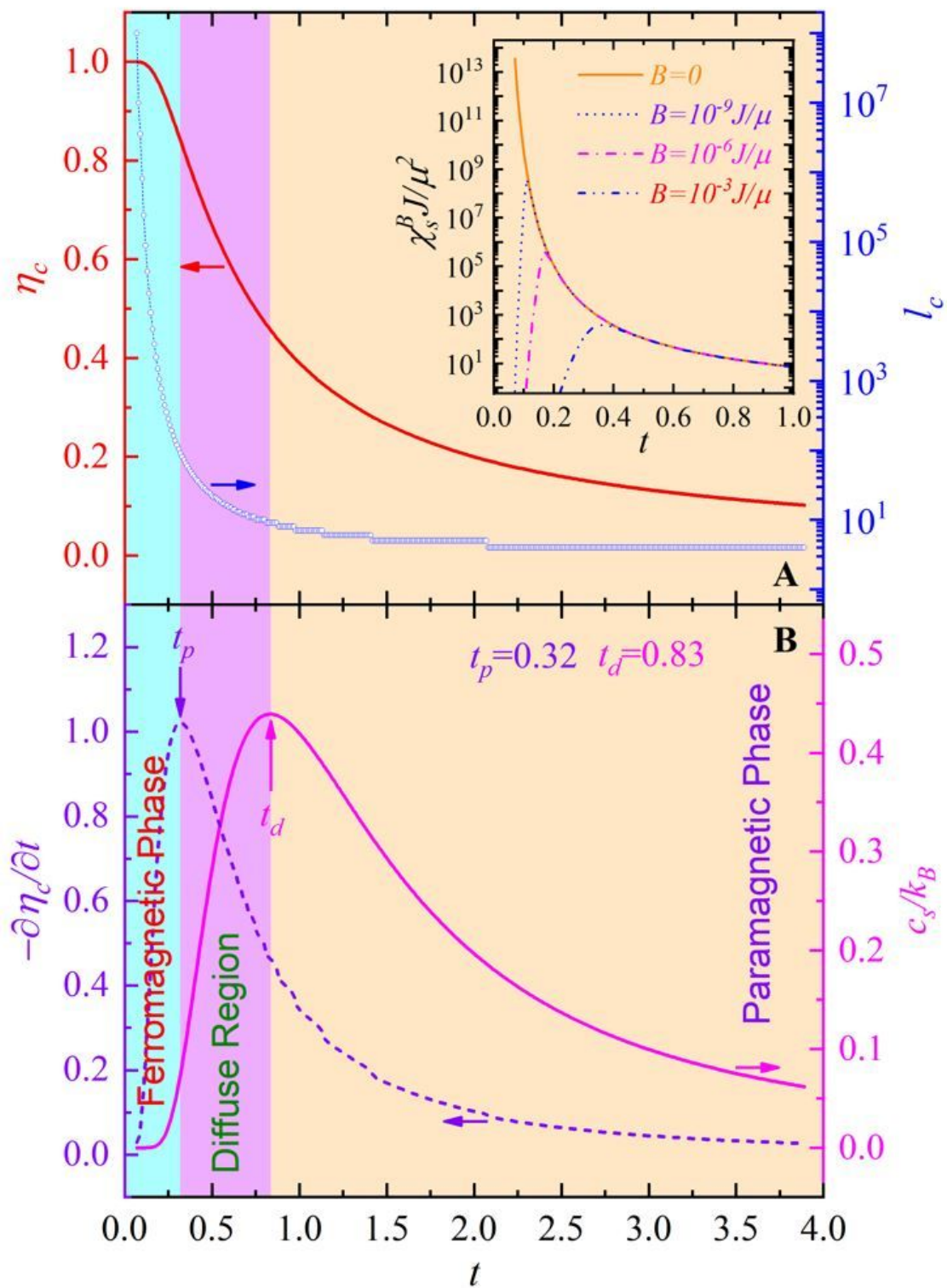


Figure 2

Please see the Manuscript file for the complete figure caption.

Supplementary Files

This is a list of supplementary files associated with this preprint. Click to download.

- [CommPhys1DIMSI20210506.docx](#)
- [CommPhys1DIMSI20210506.docx](#)